ADVANCES IN ATMOSPHERIC SCIENCES, VOL. 31, MARCH 2014, 385–395

The Limiting Effect of Deep Soil Water on Evapotranspiration of a Subtropical Coniferous Plantation Subjected to Seasonal Drought

TANG Yakun[1,2], WEN Xuefa*[1], SUN Xiaomin[1], ZHANG Xinyu[1], and WANG Huimin[1]

[1]*Key Laboratory of Ecosystem Network Observation and Modeling, Institute of Geographic Sciences and Natural Resources Research, Chinese Academy of Sciences, Beijing* 100101

[2]*University of Chinese Academy of Sciences, Beijing* 100049

(Received 8 January 2013; revised 27 May 2013; accepted 4 July 2013)

ABSTRACT

Seasonal drought is a common occurrence in humid climates. The year 2003 was the driest year during the period 1985–2011 in southeastern China. The objective of this study was to elucidate the impact of the exceptional drought in 2003, compared with eddy flux measurements during 2004–11, on the dynamics of evapotranspiration (ET) and related factors, as well as their underlying mechanisms, in a subtropical coniferous plantation in southeastern China. It was found that daily ET decreased from 5.34 to 1.84 mm during the intensive drought period and recovered to 4.80 mm during the subsquent recovering drought period. Path analysis indicated that ET was mainly determined by canopy conductance and deep soil water content (50 cm) during the intensive drought and recovering drought periods, respectively. The canopy conductance offset the positive effect of air vapor pressure deficit on ET when suffering drought stress, while the canopy conductance enhanced the positive effect of air temperature on ET during the late growing season. Because the fine roots of this plantation are mainly distributed in shallow soil, and the soil water in the upper 40 cm did not satisfy the demand for ET, stomatal closure and defoliation were evident as physiological responses to drought stress.

Key words: ChinaFLUX, evapotranspiration, seasonal drought, subtropical coniferous plantation

Citation: Tang, Y. K., X. F. Wen, X. M. Sun, X. Y. Zhang, and H. M. Wang, 2014: The limiting effect of deep soil water on evapotranspiration of a subtropical coniferous plantation subjected to seasonal drought. *Adv. Atmos. Sci.*, **31**(2), 385–395, doi: 10.1007/s00376-013-2321-y.

1. Introduction

The occurrence of drought in the Northern Hemisphere is characterized by decreased rainfall and an altered precipitation regime (IPCC, 2007). The definition of drought falls into four categories: meteorological, hydrological and agricultural droughts that occur as physical phenomena, as well as socioeconomic drought in terms of water supply and demand (Mishra and Singh, 2010). The Palmer drought severity index (PDSI), Budyko's aridity index (AI), Relative extractable water (REW) and other indexes have been used to characterize the occurrence, duration and end of a drought period (Budyko, 1974; Kumagai et al., 2004; Mishra and Singh, 2010). For example, the AI is given as the ratio of precipitation (P) to potential evapotranspiration and is widely used as a drought index (Budyko, 1974; Jassal et al., 2009).

Forest evapotranspiration (ET) accounts for approximately 45% of the ET in terrestrial ecosystems and plays a key role in water and energy balance (Flanagan et al., 2002). ET is also an important ecosystem process variable closely related to energy distribution, stomatal conductance, the carbon budget, and water use efficiency (WUE) (Wilson and Baldocchi1, 2000). Predicting the interaction between forest ecosystems and climate change requires a solid understanding of the impact of seasonal drought as an intermittent disturbance on the water cycle and its underlying mechanism. Currently, few studies have been conducted on the effects of drought in humid climates (Costa et al., 2010).

The few published studies on the impact of seasonal drought on forest ET in humid climates have focused mainly on tropical rainforests and forests in the southern United States, Western Europe, Mediterranean climate areas, and Southeast Australia (Goldstein et al., 2000; Leuning et al., 2005; Costa et al., 2010); we are not aware of any research on the impact of drought stress on forest ET in subtropical forests in East Asia. The published studies on seasonal drought in humid climates have examined forest ET and related factors, such as the Bowen ratio (β), the ratio of latent heat to net radiation ($\lambda E/R_{\rm n}$), the Priestley–Taylor coefficient (α) (Goldstein et al., 2000; da Rocha et al., 2004; Li et al., 2010), the decoupling coefficient

* Corresponding authors: WEN Xuefa
Email: wenxf@igsnrr.ac.cn

(Ω) (Kumagai et al., 2004; Bracho et al., 2008), and WUE (Jassal et al., 2009). The environmental and physiological mechanisms underlying these parameters have also been analyzed. WUE is usually measured as the ratio of gross ecosystem photosynthesis (GEP) to ET ($WUE_{\_GEP}$) and as the ratio of net ecosystem production (NEP) to ET ($WUE_{\_NEP}$).

The responses of forest ET to seasonal drought and its controlling mechanisms are diverse in humid climate areas (Bracho et al., 2008; Costa et al., 2010); they are not only related to forest ecosystem types and their water use strategies (Baldocchi et al., 2004; Hernández-Santana et al., 2008), but are also influenced by the soil water supply capacity (Bracho et al., 2008; Costa et al., 2010). When suffering from drought stress, a declining stage (Goldstein et al., 2000; Malhi et al., 2002), stable stage (Kumagai et al., 2004; Bracho et al., 2008; Li et al., 2010), and even an increasing stage (Costa et al., 2010) of forest ET can be observed relative to non-drought periods. Drought stress alters the interaction between environmental and physiological factors, and this interaction determines the seasonal variation of ET (Wilson and Baldocchi1, 2000). Compared with ET, the seasonal variation and controlling mechanisms of energy distribution and WUE under drought stress also exhibit discrepancies, as these factors depend on relative changes between ET and other flux variables, such as the sensible heat flux and carbon dioxide (CO_2) assimilation (Malhi et al., 2002; Jassal et al., 2009).

China has a forest area of 175 million ha, or 18% of the national land size, and plantations account for 31.5% of the total forest area (CFA, 2005). Of the plantation forests in China, 42% are distributed in the subtropical region (CFA, 2005). This area is characterized by abundant water and energy resources supplied by the subtropical East Asian monsoon. However, drought stress occurs because of the out-of-step relationship between temperature and precipitation in summer, which is associated with a Pacific subtropical high pressure system (Dairaku et al., 2008). In southeastern China, seasonal drought generally starts in early July and terminates in mid-September. The year 2003 was the driest year according to meteorological records during 1985–2011. Previous research based in the plantation used for the present study has focused mainly on the impact of drought stress on the carbon exchange process (Saigusa et al., 2010; Wen et al., 2010). The response of forest ET and related factors to drought stress have yet to be investigated.

The objective of the present reported study was to elucidate the impacts of the severe drought of 2003, compared with eddy flux measurements during 2004–11, on the ET and related factors, including β, $\lambda E/R_n, a, \Omega$, $WUE_{\_GEP}$, and $WUE_{\_NEP}$, and their underlying mechanisms, in a plantation in southeastern China. We hypothesized that, being even-aged and having a shallow fine rooting system, the studied plantation would only have access to water in the shallow soil layers and that drought stress would be caused by ET demand exceeding water storage in this part of the soil profile.

2. Materials and methods

2.1. *Site description*

The plantation site used for the present study was Qianyanzhou, a member of ChinaFLUX, an observation and research network comprising 46 sites in total throughout China. The site is located within Qianyanzhou Station of the Chinese Ecosystem Research Network (CERN) (26°44′52″N, 115°03′47″E; a.s.l. 102 m) and is situated in an area under the influence of the subtropical East Asian monsoon climate. The annual average temperature and precipitation amount are 17.0°C and 1355 mm, respectively, according to meteorological records during 1985–2011. The maximum and minimum annual precipitation amounts during that period were 2410 mm in 2002 and 945 mm in 2003, respectively.

The flux tower is located in the foothills with a slope ranging from 2.8° to 13.5°. The plantation was established in 1985, and the dominant tree species are Masson pine (*Pinus massoniana* L.), Chinese fir (*Cunninghamia lanceolata* L.) and slash pine (*Pinus elliottii* E.). The plantation has a maximum leaf area index (LAI) of 5.6 m^2 m^{-2}, which was recorded using an LI-2000 leaf area meter (Model LI-2000, Licor Inc.). In 2004, the mean height of Masson pine, Chinese fir and slash pine was 9.5, 10.9, and 12.0 m, respectively, with mean diameters at breast height of 13.1, 13.2, and 15.8 cm, respectively, and stem densities of 444, 210, and 809 stems ha^{-1}, respectively. The soil type is red earth with red sandstone and mud stone as the parent material. Further information on the study site is provided in Wen et al. (2010).

2.2. *Eddy covariance and meteorological measurements*

An eddy covariance system was mounted on a tower at 39.6 m. It consisted of an LI-7500 open-path CO_2/H_2O analyzer (Model LI-7500, Licor Inc.) and a three-dimensional sonic anemometer (Model CSAT3, Campbell Scientific Inc.). Flux variables were sampled at 10 Hz using a CR5000 datalogger (Model CR5000, Campbell Scientific Inc.), and 30-min mean fluxes were calculated.

Air temperature and relative humidity sensors (Model HMP45C, Vaisala Inc.) as well as wind speed sensors (A100R, Vector Inc.) were mounted at heights of 1.6, 7.6, 11.6, 15.6, 23.6, 31.6, and 39.6 m above ground. A four-component net radiometer (Model CNR-1, Kipp & Zonen Inc.), a quantum sensor of photosynthetically active radiation (Model LI190SB, Licor Inc.), and a pyranometer (Model CM11, Kipp & Zonen Inc.) were used to measure radiation. Soil temperatures were measured at depths of 2, 5, 20, 50, and 100 cm using thermocouples (105T and 107-L, Campbell Scientific Inc.), and the soil volumetric water contents were recorded at depths of 5, 20, and 50 cm using three TDR probes (Model CS615-L, Campbell Scientific Inc.). Precipitation was monitored using a rain gauge (Model 52203, RM Young Inc.). The meteorological data were sampled at 1 Hz with 30-min averages collected by three CR10X dataloggers (Model CR10XTD, Campbell Scientific Inc.) and a CR23X datalogger (Model CR23XTD, Campbell Scien-

tific Inc.) with a 25-channel solid-state multiplexer (Model AM25T, Campbell Scientific Inc.).

2.3. *Flux correction and gap filling*

The ET (g H_2O m^{-2} s^{-1}) and NEP (mg CO_2 m^{-2} s^{-1}) between the forest and atmosphere were calculated as follows:

$$\mathrm{ET} = \overline{w'\rho_v'(z_r)} + \rho \sum_{i=1}^{n} [(\Delta e_i/\gamma\Delta t)\Delta z_i] \,, \quad (1)$$

$$\mathrm{NEP} = \overline{w'\rho_c'(z_r)} + \Delta\rho_c z_r/\Delta t \,. \quad (2)$$

The first term on the right-hand side is the eddy flux of the water vapor or CO_2, where w' is vertical wind speed fluctuation (m s^{-1}), ρ_v' is water vapor density fluctuation (g m^{-3}), ρ_c' is CO_2 concentration fluctuation (mg m^{-3}), z_r is the height of eddy covariance observation (m), and over-bar indicates an averaging operation. The second term is the storage of water vapor or CO_2 below z_r, where ρ is air density (g m^{-3}), ρ_c is the CO_2 concentration (mg m^{-3}), e_i is vapor pressure at the height of meteorological profile (kPa K^{-1}), γ is the psychrometric constant (kPa K^{-1}), z_i is the height of meteorological profile observation (m), and t is time (s). All advective terms in the mass conservation equation are ignored. The water vapor storage term was calculated based on the profile air temperature and relative humidity, as suggested by McCaughey (1985) and Oliphant et al. (2004). The CO_2 storage term was computed using the change in CO_2 concentration at the eddy covariance level according to Hollinger et al. (1994) and Griffis et al. (2003).

Planar fit rotation was applied to remove the effect of instrument tilt or irregularity on the airflow at monthly intervals (Wilczak et al., 2001). The Webb-Pearman-Leuning (WPL) correction was performed to correct for the effect of air density fluctuations on the water vapor and CO_2 fluxes (Webb et al., 1980). Abnormal data caused by precipitation, water condensation and system failure were eliminated. Any value that exceeded five times the standard deviation within a window of 10 values was deleted. To obtain reliable data at night, all data with a friction velocity less than 0.19 m s^{-1} were rejected (Wen et al., 2010). Negative NEP fluxes at nighttime (i.e., apparent "photosynthesis") were also removed from the datasets. Data gaps were produced as a result of these data omissions. From 2003–11, the average daytime and nighttime reliable data coverage was 81% and 25% for ET, respectively, and 76% and 20% for NEP, respectively.

Missing micrometeorological data with gaps less than 2 h were interpolated linearly from adjacent data points, and those with gaps longer than 2 h were interpolated using the meteorological data from a nearby meteorological station. Missing water vapor flux and CO_2 data were interpolated linearly from adjacent values when gaps were less than 2 h. Water vapor flux data with gaps longer than 2 h were interpolated using a look-up table method (Falge et al., 2001). Daytime CO_2 flux data (NEP) with gaps longer than 2 h were estimated using the Michaelis–Menten equation with an independent 10-day window (Falge et al., 2001). Nighttime CO_2 flux data (RE_{night}, ecosystem respiration) with gaps longer than 2 h were estimated as a function of soil temperature and soil water content using the equation suggested by Reichstein et al. (2002) with a yearly window. To estimate GEP (GEP = NEP + RE), daytime ecosystem respiration (RE_{day}, ecosystem respiration) was estimated by extrapolating the nighttime relationship function of the ecosystem respiration (RE_{night}) with soil temperature and soil water content.

2.4. *Calculation of bulk canopy parameters*

In this study, the daytime values of canopy conductance, the Priestley–Taylor coefficient (α), and the decoupling coefficient (Ω) were obtained by averaging the half-hourly values from 1000–1600 LST for days with data coverage greater than 80%. The bulk canopy parameters on rainy days (0000–1600 LST) were excluded from the analysis. Here, canopy conductance is the weighted integration of the conductance of an individual leaf, and is a physiological index that responds to environmental conditions (Wilson and Baldocchi1, 2000). The canopy conductance (g_c) is computed by inverting the Penman–Monteith equation (Monteith and Unsworth, 1990):

$$g_c = (\gamma\lambda E g_a)/[s(R_n - G) + \rho c_p \mathrm{VPD} - \lambda E(s+\gamma)] \,, \quad (3)$$

$$g_a = [(u/u^{*2}) + 6.2u^{*-0.67}]^{-1} \,. \quad (4)$$

Here, R_n is the net radiation (W m^{-2}), G is the soil heat flux (W m^{-2}), s is the slope of the function relating the saturation vapor pressure to temperature (kPa K^{-1}), λE is the latent heat flux (W m^{-2}), c_p is the specific heat of air (J kg^{-1} K^{-1}), VPD is the air vapor pressure deficit (kPa), ρ is the air density (kg m^{-3}), g_a is the aerodynamic conductance (mm s^{-1}), u is the wind speed (m s^{-1}), and u^* is the friction velocity (m s^{-1}).

The Priestley–Taylor coefficient (a) is considered to be the ratio of measured ET to climatologically expected ET (equilibrium ET, ET_{eq}), the latter of which assumes a closed air volume with abundant net radiation over a "wet" surface (McNaughton and Spriggs, 1986). The Priestley–Taylor coefficient (α) is computed as follows:

$$\alpha = \mathrm{ET}/\mathrm{ET}_{eq} \,, \quad (5)$$

$$\mathrm{ET}_{eq} = [(R_n - G)s]/(s+\gamma) \,. \quad (6)$$

The decoupling coefficient (Ω) indicates the magnitude of the coupling between the vegetation and atmosphere and ranges from 0 to 1 (Jarvis and McNaughton, 1986). The coupling characteristic between the vegetation and the atmosphere is controlled by canopy conductance if Ω approaches 0 and by net radiation and temperature if Ω approaches 1:

$$\Omega = (s/\gamma + 1)/(s/\gamma + 1 + g_a/g_c) \,. \quad (7)$$

2.5. *Path analysis*

Path analysis is an extension of multiple regression. Schemske and Horvitz (1988) and Huxman et al. (2003) briefly explain the mechanism of path analysis as follows: the direct path coefficient between the independent and dependent variable is the standardized partial-regression coefficient

of their first multiple regression, and the indirect path coefficient is the product of the standardized partial-regression coefficients summed across all possible paths. The total causal coefficient is the sum of the direct and indirect coefficient. Thus, the path coefficient may represent the direct or indirect, or the sum of direct and indirect, controlling effects of an independent variable with respect to a dependent variable (Huxman et al., 2003). A path coefficient of 1 means complete causality, and 0 means no causality. A positive value indicates positive effect, and vice versa.

In our study, the initial list of environmental and physiological variables used in path analysis included the net radiation, air temperature, air vapor pressure deficit, soil water content at depths of 5 cm, 20 cm, and 50 cm (S_w_5cm, S_w_20cm, and S_w_50cm) and canopy conductance. In order to ensure the reliability of the path analysis, a stepwise multiple regression analysis was first adopted to select significant independent variables ($p < 0.05$). Then, the Pearson product-moment correlation coefficient between selected independent and dependent variables was used to detect the possibility of significant correlation of each variable ($p < 0.05$). The aforementioned statistical analysis was performed using SPSS (2004, ver.13.0; SPSS Inc.). Subsequently, the path analysis was run for selected variables using Amos (2003, ver.5.0; SPSS Inc.) to interpret the direct and indirect controlling mechanisms of these independent variables on ET and related factors. All insignificant paths ($p > 0.05$) and ecological nonsense paths were deleted from our path diagram.

2.6. *Remotely-sensed vegetation index*

As the enhanced vegetation index (EVI) is more resistant to soil background and less susceptible to atmospheric disturbance, this remotely-sensed vegetation index has been widely used as an indicator to detect vegetation ecosystem suffering from drought stress (Churkina et al., 2005; Zhang et al., 2011). The 8-day EVI at a spatial resolution of 500 m used in this study was calculated using the method presented by Huete et al. (2002). Additionally, the MODIS/Terra Surface Reflectance 8-Day L3 Global 500 m (MOD09A1) data were obtained from the data portal at the Earth Observation and Modeling Facility at the University of Oklahoma. The Savitzky–Golay method was adopted to detect and replace abnormal EVI values (Zhang et al., 2011); a window length parameter of four was used in this method.

3. Results

3.1. *Out-of-step relationship between temperature and precipitation during summer*

Figure 1a shows the seasonal variations of the daily average air temperature and air vapor pressure deficit. The annual mean daily temperature was 18.9°C ± 0.47°C (mean ± one standard error) in 2003. Herein, spring is defined from March through May, summer from June through August, autumn from September through November, and winter from December through February. The lower air temperatures

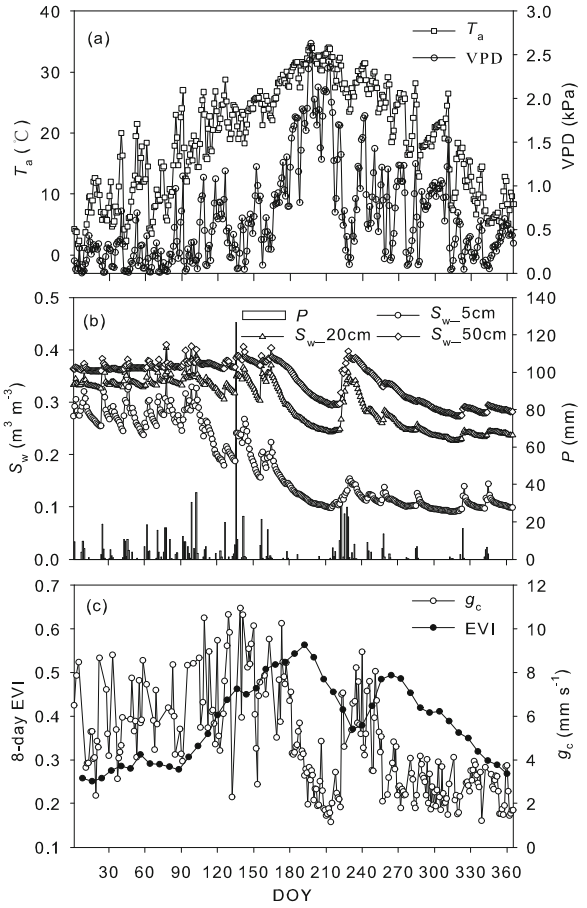

Fig. 1. Seasonal variations of (a) air temperature (T_a) and air vapor pressure deficit (VPD), (b) soil water content at depths of 5 cm, 20 cm, and 50 cm (S_w_5cm, S_w_20cm, and S_w_50cm) and precipitation (P), and (c) enhanced vegetation index (EVI) and canopy conductance (g_c) of the plantation in 2003.

occurred in winter, with a minimum daily value of −2.2°C, and the highest daily air temperature occurred in the summer (up to 34.4°C). The air vapor pressure deficit was closely related to air temperature, the annual mean daily air vapor pressure deficit was approximately 0.63 ± 0.03 kPa, and the minimum and maximum daily values were 0.002 kPa and 2.6 kPa, respectively.

Figure 1b shows the seasonal variations of the precipitation and soil water contents at depths of 5 cm, 20 cm and 50 cm. In general, precipitation occurred more frequently in spring than in summer and winter. The annual precipitation in 2003 was 945 mm, which was the lowest during 1985–2011 and was 70% of the 1985–2011 mean annual precipitation. The precipitation in July was approximately 3 mm, which accounted for only 0.5% of the annual total in 2003 and 2.7% of the July mean precipitation of 1985–2011. Seasonal drought stress resulted from the relatively high temperatures and lack of sufficient precipitation in July. The seasonal trend in the soil water content generally followed that of the precipitation regime. The soil water content during the first half of the year was higher than that during the latter half, with the minimum

value occurring during the seasonal drought. The magnitude of seasonal variation of the soil water content was 0.09–0.35 (0.18 ± 0.004) $m^3\ m^{-3}$, 0.23–0.40 (0.3 ± 0.003) $m^3\ m^{-3}$, and 0.27–0.41 (0.34 ± 0.002) $m^3\ m^{-3}$ at depths of 5, 20, and 50 cm, respectively. These magnitudes decreased with increasing soil depth.

Figure 1c shows the seasonal variations of canopy conductance and the 8-day EVI. The annual mean canopy conductance was 4.56 ± 0.15 mm s^{-1} with a variation of 1.14–10.95 mm s^{-1}. The canopy conductance increased over time in spring to early summer with a gradually enhanced physiological activity, but then dramatically decreased due to the intensive summer drought. With the occurrence of precipitation in August, the canopy conductance increased again during the recovering drought period. In autumn and winter, the canopy conductance decreased with time, coincident with the gradual attenuation of physiological activity. Although the seasonal variation of EVI was consistent with that of canopy conductance, there was an approximate 19-day phase lag of EVI relative to canopy conductance during the summer drought.

3.2. *Drought effects on the seasonal variation of ET*

Figure 2 shows the seasonal variations of monthly AI and 7-day running-mean ET in 2003 and 2004–11. An AI value of less than 1 indicates water-limited conditions (Budyko, 1974; Jassal et al., 2009). The lowest AI value was 0.04 in July 2003, which was much smaller than the mean value of 1.03 in the same month during 2004–11. Thus, July in 2003 was considered to have experienced severe drought stress (Fig. 2a).

The ET in 2003 was clearly below the range of that observed in 2004–11 during the seasonal drought (Fig. 2b), which was indicative of the inconsistent distribution of temperature and precipitation in summer. The ET in 2003 shows a bimodal curve characteristic, with lower values during the summer drought and winter, which could be divided into non-drought periods, including the early [day of year (DOY) 1–182)] and late (DOY 238–365) growing periods, and seasonal drought periods, including intensive drought (DOY 183–214) and recovering drought periods (DOY 215–237). The annual sum of ET was 772 mm, with a daily sum in the range of 0.33–5.34 mm. During the early growing period, ET increased gradually and reached a peak value of 5.34 mm d^{-1}. However, ET decreased by 66% to 1.84 mm d^{-1} during the intensive drought period. During the subsequent recovering drought period, ET increased to 4.80 mm d^{-1}, while ET decreased again due to decreased plant physiological activities and atmospheric demand during the late growing period.

The $\lambda E/R_n$ (Fig. 3a), α (Fig. 3b), Ω (Fig. 3d), and $WUE_{\_NEP}$ (Fig. 4b) values showed seasonal trends similar to that of ET, while β (Fig. 3c) and $WUE_{\_GEP}$ (Fig. 4a) showed an inverse trend. It is important to note that during the seasonal drought period, $WUE_{\_NEP}$ and $WUE_{\_GEP}$ in 2003 were clearly below the range of the $WUE_{\_NEP}$ observed in 2004–11 (Fig. 4). An unexpected declined in $WUE_{\_NEP}$ was observed as heavy precipitation occurred (DOY 228–230) during the recovering drought period. The annual mean values of

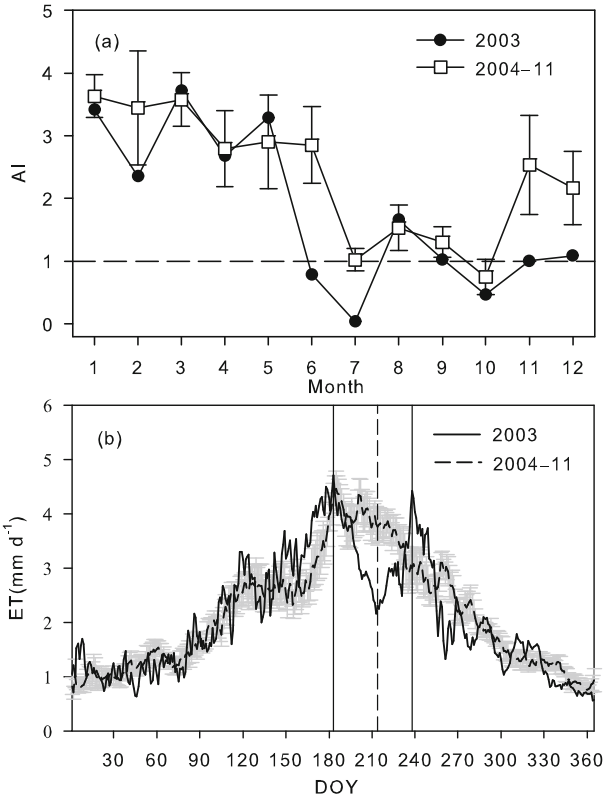

Fig. 2. Seasonal variations of the (a) monthly Budyko's aridity index (AI) and (b) 7-day running-mean of ET in 2003 and during 2004–11 of the plantation. The error bars indicate one standard error. Vertical solid lines and the dashed line in (b) indicate the boundary between the non-drought and seasonal drought periods, and between the intensive drought and recovering drought periods, respectively.

$\lambda E/R_n$, α, Ω, β, $WUE_{\_NEP}$, and $WUE_{\_GEP}$ were 0.61 ± 0.01, 0.57 ± 0.03, 0.32 ± 0.01, 0.68 ± 0.03, 0.59 ± 0.03 g C kg^{-1} H_2O d^{-1}, and 2.50 ± 0.06 g C kg^{-1} H_2O d^{-1}, respectively.

Relative to ET, the variations of $\lambda E/R_n$, α, Ω, and β showed a phase-advance of several days during the intensive drought period, while the variations of $WUE_{\_NEP}$ and $WUE_{\_GEP}$ showed a phase-lag of several days. The reason for these shifts was that the increasing trend of ET was less than those of $\lambda E/R_n$, α, Ω, and β (Fig. 3) and higher than those of $WUE_{\_NEP}$ and $WUE_{\_GEP}$. No phase difference was observed during the recovering drought period.

3.3. *Environmental and physiological mechanisms of ET under seasonal drought*

Figure 5 demonstrates the direct and indirect causality of environmental factors and canopy conductance in the control of ET during the non-drought and seasonal drought periods. The equations of path analysis of ET and related factors are listed in Table 1 for these periods. Only the controlling factors that reached the level of statistical significance ($p < 0.05$) were adopted in the path analysis. During the intensive drought period, the dynamics of ET was mainly controlled by canopy conductance with a direct path coefficient

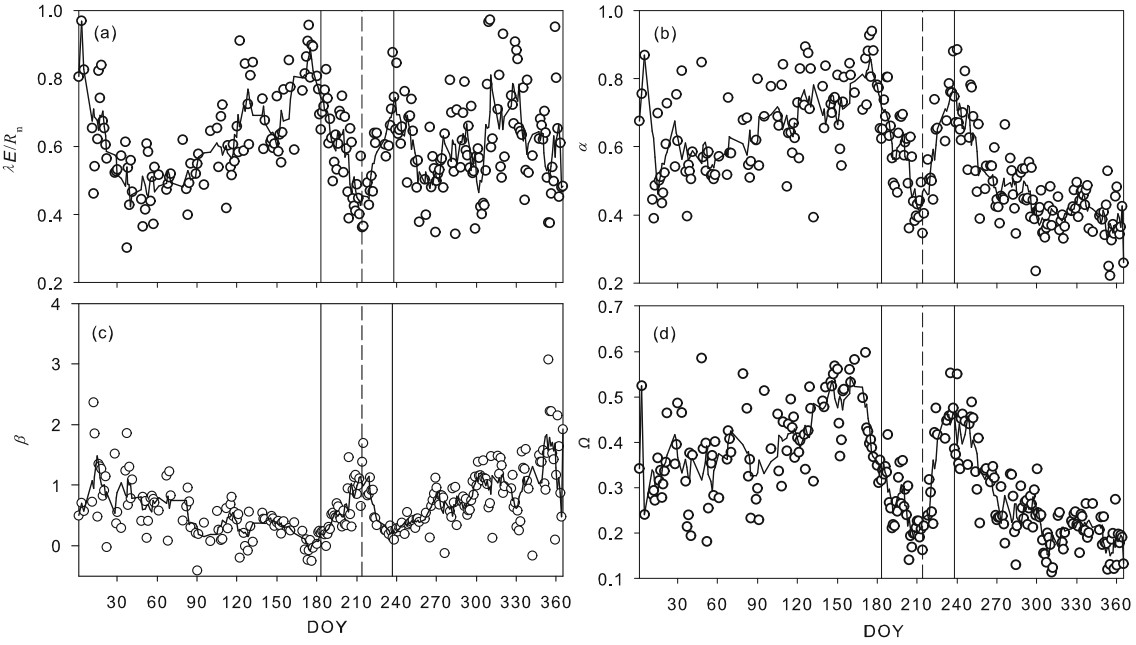

Fig. 3. Seasonal variations of the daily and 7-day running-mean of (a) the ratio of latent heat to net radiation ($\lambda E/R_n$), (b) Priestley–Taylor coefficient (α), (c) Bowen ratio (β), and (d) decoupling coefficient (Ω) of the plantation in 2003. The same non-drought and drought periods in Fig. 2b are shown for comparison. Daily α and Ω values were calculated by averaging all available half-hourly values from 1000–1600 LST.

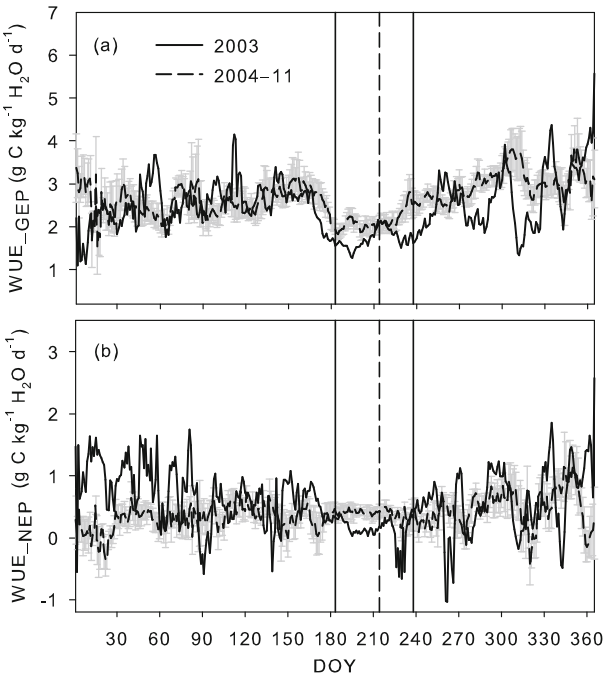

Fig. 4. Seasonal variations of the 7-day running-mean of water use efficiency (a) $WUE_{\_GEP}$ (GEP/ET) and (b) $WUE_{\_NEP}$ (NEP/ET) in 2003 and during 2004–11 of the plantation. The error bars indicate one standard error. The same non-drought and drought periods in Fig. 2b are shown for comparison.

of 0.96 (Fig. 5b). The values of $\lambda E/R_n$ and α were primarily dominated by soil water content at 50 cm with a total path coefficient both of 0.77 (Table 1). The $\lambda E/R_n$ and α values were also positively and directly dependent on canopy conductance. The air vapor pressure deficit not only had a direct positive control on ET, $\lambda E/R_n$, and α, but also indirectly controlled these factors through its negative effect on canopy conductance. Furthermore, the air vapor pressure deficit indirectly controlled ET through its negative effect on shallow soil water content (S_w_5cm) (Fig. 5b). These negative relationships offset the direct coefficient of air vapor pressure deficit, ultimately reducing its direct path coefficient from 0.51 to a total coefficient of -0.25 for ET (Fig. 5b, Table 1), from 0.33 to a total coefficient of 0.13 for $\lambda E/R_n$ and from 0.31 to a total coefficient of 0.08 for α (Table 1). This offsetting effect between physiological and environmental factors can be considered as the protective mechanism of the forest to cope with drought stress (Wilson and Baldocchi1, 2000). The value of β was mainly controlled by soil water content at a depth of 20 cm; canopy conductance also offset the negative direct effect of air vapor pressure deficit on β. The net radiation and soil water content at a depth of 20 cm were dominated $WUE_{\_GEP}$ and $WUE_{\_NEP}$ with total coefficients of -0.54 and 0.55, respectively (Table 1).

During the recovering drought period, the soil water content at a depth of 50 cm played a direct key role in controlling ET and β, with direct path coefficients of 0.61 and -0.86, respectively. $\lambda E/R_n$ and α were dominated by canopy conductance, with direct path coefficients of 0.81 and 0.91, respectively (Table 1). $WUE_{\_NEP}$ was mainly dominated by canopy conductance, while there was no significant control of $WUE_{\_GEP}$ by any of the aforementioned environmental and physiological factors.

During the non-drought periods, the prevailing factors controlling ET, β, $\lambda E/R_n$, α, $WUE_{\_GEP}$, and $WUE_{\_NEP}$ were diverse (Table 1). During the early growing period, the

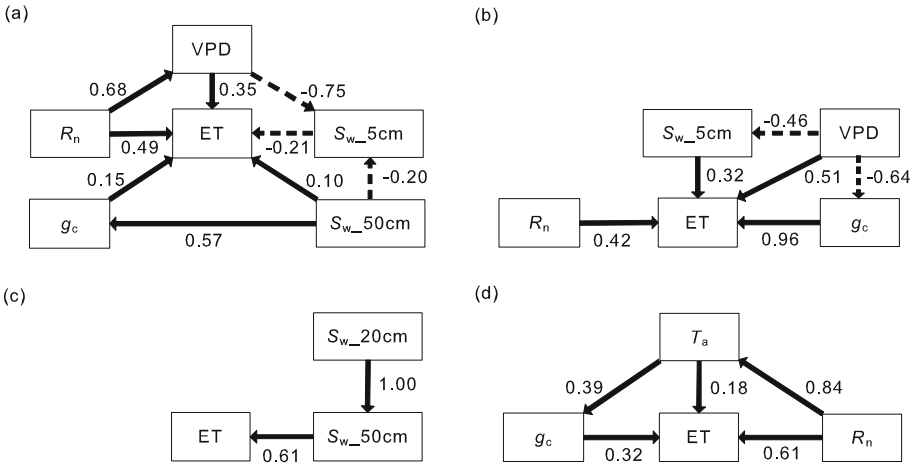

Fig. 5. The direct and indirect causality of the net radiation (R_n), air temperature (T_a), vapor pressure deficit (VPD), soil water content at depths of 5 cm, 20 cm, and 50 cm (S_w_5cm, S_w_20cm, and S_w_50cm), and canopy conductance (g_c) in the control of ET during the (a) early and (d) late growing periods, and the (b) intensive and (c) recovering drought periods of the plantation in 2003. Solid and dashed arrows represent positive and negative correlations, respectively.

Table 1. The path analysis equations of net radiation (R_n), air temperature (T_a), vapor pressure deficit (VPD), soil water content at depths of 5 cm, 20 cm, and 50 cm (S_w_5cm, S_w_20cm, and S_w_50cm), and canopy conductance (g_c) in the control of ET, the Bowen ratio (β), the ratio of latent heat to net radiation ($\lambda E/R_n$), the Priestley–Taylor coefficient (α), $WUE_{\_GEP}$ (GEP/ET), and $WUE_{\_NEP}$ (NEP/ET) during the early (DOY 1–182) and late (DOY 238–365) growing periods, and the intensive (DOY 183–214) and recovering (DOY 215–237) drought periods. The "-" sign indicates no significant independent variables ($p < 0.05$).

Period	Equations	r^2	p	N
Early growing period	$ET = 0.83R_n + 0.51VPD - 0.23S_w\_50cm - 0.21S_w\_5cm + 0.15g_c$	0.92	< 0.01	92
	$\beta = -0.62T_a - 0.18g_c$	0.42	< 0.05	92
	$\lambda E/R_n = -0.53S_w\_5cm + 0.44VPD + 0.29g_c + 0.04R_n$	0.38	< 0.05	92
	$\alpha = 0.63VPD + 0.59S_w\_50cm + 0.52g_c - 0.11R_n$	0.76	< 0.001	92
	$WUE_{\_GEP} = -0.97VPD - 0.26T_a$	0.35	< 0.01	92
	$WUE_{\_NEP} = -0.99T_a - 0.32VPD - 0.22R_n$	0.51	< 0.05	92
Intensive drought period	$ET = 0.96g_c + 0.42R_n + 0.32S_w\_5cm - 0.25VPD$	0.86	< 0.01	31
	$\beta = -0.80S_w\_20cm + 0.50R_n - 0.39g_c - 0.02VPD$	0.89	< 0.05	31
	$\lambda E/R_n = 0.77S_w\_50cm + 0.52g_c - 0.45R_n + 0.13VPD$	0.89	< 0.001	31
	$\alpha = 0.77S_w\_50cm + 0.58g_c - 0.43R_n + 0.08VPD$	0.88	< 0.001	31
	$WUE_{\_GEP} = -0.54R_n - 0.28S_w\_5cm - 0.22VPD$	0.41	< 0.05	31
	$WUE_{\_NEP} = 0.55S_w\_20cm + 0.22g_c$	0.32	< 0.001	31
Recovering drought period	$ET = 0.61S_w\_50cm + 0.60S_w\_20cm$	0.37	< 0.001	15
	$\beta = -0.86S_w\_50cm$	0.74	< 0.001	15
	$\lambda E/R_n = 0.81g_c$	0.65	< 0.001	15
	$\alpha = 0.91g_c$	0.91	< 0.001	15
	$WUE_{\_GEP}$	-	-	15
	$WUE_{\_NEP} = 0.60g_c$	0.36	< 0.001	15
Late growing period	$ET = 0.87R_n + 0.32g_c + 0.31T_a$	0.87	< 0.001	102
	$\beta = 0.60VPD - 0.50T_a - 0.25g_c$	0.43	< 0.01	102
	$\lambda E/R_n = 0.45g_c - 0.41VPD$	0.37	< 0.01	102
	$\alpha = 0.70g_c + 0.60T_a + 0.45S_w\_50cm + 0.17R_n$	0.76	< 0.01	102
	$WUE_{\_GEP} = -0.53T_a$	0.28	< 0.05	102
	$WUE_{\_NEP} = -0.76T_a - 0.10R_n$	0.18	< 0.05	102

value of ET was mainly determined by net radiation; β and $WUE_{\_NEP}$ were controlled by air temperature. The air vapor pressure deficit was the main contributor to α and $WUE_{\_GEP}$. The soil water content at 5 cm played a key role in controlling $\lambda E/R_n$. During the late growing period, with the exception of $\lambda E/R_n$ and α, which were determined by canopy conductance, ET and β were mainly dominated by net radiation and the air vapor pressure deficit, respectively. $WUE_{\_GEP}$ and $WUE_{\_NEP}$ were both controlled by air temperature (Table 1). It is important to note that there was no relationship between air vapor pressure deficit and canopy conductance during the non-drought period. The canopy conductance enhanced the controlling mechanism of air temperature on β during the early growing period and on ET and α during the late growing period.

4. Discussion

4.1. *Effects of canopy conductance and soil water content on ET during seasonal drought*

Previous studies have demonstrated that decreased canopy conductance and soil water content are not always followed by decreased ET (da Rocha et al., 2004; Li et al., 2010). This result is mainly due to the uptake of deep soil water by the root system, which is sufficient to maintain forest ET (Leuning et al., 2005; Bracho et al., 2008). For example, although canopy conductance declined somewhat, the ET values of a tropical rain forest in southern China (Li et al., 2010), and an oak forest and pine forest in the southern United States (Bracho et al., 2008), have been found to maintain normal rates under drought stress. In addition, the ET of an Amazon tropical rainforest during a drought period has been observed to exceed that during a non-drought period (Costa et al., 2010).

However, our study shows that not all forests can maintain unabated ET during seasonal drought. At our site, both canopy conductance and ET declined during the drought event. Similar results during seasonal drought have been reported for a rainforest in the Amazon (Costa et al., 2010) and for a deciduous forest in the southern United States (Wilson and Baldocchi1, 2000). In our case, it is noteworthy that canopy conductance and deep soil water content were the main contributors to ET dynamics during the intensive and recovering drought period (Figs. 5b and c), respectively, indicating that the amount of soil water in the shallow depths of 5 cm and 20 cm did not satisfy the demand for ET.

Granier et al. (2007) reported that drought stress can be relieved by precipitation events. During the recovering drought period, ET, $\lambda E/R_n$, α, and canopy conductance rapidly recovered in this plantation forest, meaning that drought stress did not cause the majority of premature mortality of roots or twigs as in a study in Western Europe (Bréda et al., 2006). However, a time delay effect of precipitation replenishing deep soil content should also be considered, as the deep soil water content (50 cm) was the dominant contributor to ET during the recovering drought period.

4.2. *Plant strategies to cope with seasonal drought*

Previous studies have demonstrated that stomatal closure, defoliation, tapping into deeper sources of soil water, or hydraulic lift are strategies that plant species have adapted to deal with drought stress (Baldocchi et al., 2004; Costa et al., 2010). When affected by short-term drought stress, plants invoke physiological adjustments, such as stomatal closure, to prevent the leaf water potential from dropping below a critical level (Hernández-Santana et al., 2008). In this study, the canopy conductance decreased as air vapor pressure deficit increased and could be viewed as one of strategies the forest used to adapt to the drought stress. Decreased canopy conductance can offset the enhanced effect of air vapor pressure deficit on ET, $\lambda E/R_n$, and α. Other adaptive strategies could also include defoliation.

There was a 19-day phase lag between the decline in EVI relative to the decline in canopy conductance, thereby illustrating a delayed effect between stomatal closure and defoliation during the intensive drought period, as well as the revival of vegetation during the recovering drought period. This defoliation phenomenon was confirmed by our monthly litter measurements of the dominant trees. In July (DOY 182–212) and August (DOY 213–243) in 2003, the litter fall was 41.25 and 64.84 g m^{-2}, respectively, which was 2.8 and 2.2 times more than the July and August monthly averages, respectively, during 2004–07. The phase-lag phenomenon in this plantation was similar to that observed in an oak forest, which showed a characteristic use of stomatal closure and defoliation to adapt to drought stress (Hernández-Santana et al., 2008), but differed from forests that have the ability to tap into deep soil water sources (Migliavacca et al., 2009) or to remediate soil moisture deficits via hydraulic lift (Ishikawa and Bledsoe, 2000).

At our site, the fine roots of the dominant trees were mostly distributed between the depths of 20–30 cm, and mainly in the upper 40 cm (Fig. 6). The soil moisture dropped rapidly at this rooting depth, but not in the deeper layer during the drought event (Fig. 1c), suggesting that the fine roots performed most of the water uptake to sustain ET. Furthermore, being uniform in age and rooting distribution, this plantation forest does not have the capacity to redistribute water via hydraulic lift.

4.3. *Impact of drought on the energy distribution and decoupling characteristic*

Drought affects the stomatal conductance of vegetation and results in changes in latent and sensible heat exchange properties (Wilson and Baldocchi1, 2000; Liu et al., 2008). Drought stress also altered the energy distribution regimes (Fig. 3a), and β reached 1.70, even during the growing season in this plantation (Fig. 3c). During the intensive drought period, the sensible heat flux dominated the radiation energy partition. The latent heat flux gradually dominated the energy distribution again during the recovering drought period.

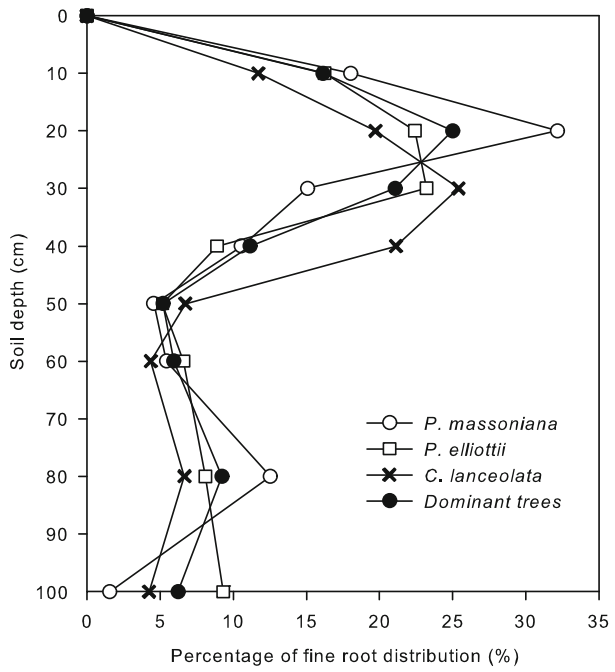

Fig. 6. The percentage of fine root distribution of *P. massoniana*, *C. lanceolata*, *P. elliottii*, and dominant trees at different soil depths of the plantation.

Similar to our plantation, the β of a ponderosa pine plantation in Sierra Nevada in the United States was higher than 1 when affected by drought stress (Goldstein et al., 2000). However, in a tropical rain forest in the Amazon suffering from drought stress, no obvious effect on β was found (da Rocha et al., 2004). On an annual scale, the annual mean value of 0.68 was higher than that of deciduous forests (0.42), but lower than that of coniferous forests (1.07) and of forests in Mediterranean climates (1.79) (Wilson et al., 2002).

In this plantation, drought enhanced the coupling efficiency between the forest and the atmosphere. The majority of the Ω values in this study were less than 0.5, thus indicating that ET was highly sensitive to physiological variability. Drought caused Ω to approach the lowest value (0.14). The annual mean value of Ω was 0.32, which was slightly higher than 0.21 reported for a cypress forest in Japan (Kosugi et al., 2007) and 0.24 for a Douglas fir forest in Canada (Humphreys et al., 2003), but lower than 0.50 for a temperate deciduous forest in the southern United States (Wilson and Baldocchi1, 2000).

4.4. *Impact of drought on WUE*

As NEP depends on how GEP and RE are affected relative to each other (Reichstein et al., 2005), the response of WUE (NEP/ET and GEP/ET) to seasonal drought also differs. Zhang et al. (2011) illustrated that GEP and NEP during the 2003 drought period were below the range during 2004–08 in this plantation and that GEP was more resistant than NEP in response to drought stress. An inverse seasonal variation between $\mathrm{WUE_{\_NEP}}$ and $\mathrm{WUE_{\_GEP}}$ was observed during the seasonal drought period (Fig. 4). This was mainly attributed to the decreased trend of ET (65%), which was smaller than that of NEP (93%) but larger than that of GEP (60%) during the intensive drought period, while the increased trend of ET (161%) was also smaller than that of NEP (203%) and larger than that of GEP (65%) during the recovering drought period. The seasonal variation of $\mathrm{WUE_{\_GEP}}$ in this plantation is consistent with a deciduous boreal forest in Canada, in which a higher $\mathrm{WUE_{\_GEP}}$ was observed during seasonal drought, but different from a mixed-wood boreal forest in Canada (Brümmer et al., 2012). Furthermore, although the $\mathrm{WUE_{\_NEP}}$ of a poplar plantation in northern Italy decreased in a manner similar to our plantation, the poplar plantation declined mainly due to a decrease in NEP, while ET remained at a normal rate when suffering from drought stress (Migliavacca et al., 2009).

Our results indicated that there was no significant dominant variable for $\mathrm{WUE_{\_GEP}}$ during the recovering drought period (Table 1), which was not only related to the different controlling mechanisms of CO_2 assimilation and ET, but also due to their discrepancies in the physiological response to drought stress. The stepwise multiple analysis showed that ET was only dominated by soil water content at depths of 50 cm and 20 cm during the recovering drought period, while there were no dominant factors for GEP. This could also be attributed to different nitrogen mineralization and carboxylation processes in response to soil water stress (Jassal et al., 2009).

5. Conclusions

In the present reported study, we illustrated the impact of an exceptional drought stress event in 2003 on the dynamics of ET and related factors, as well as their underlying mechanisms, in a subtropical coniferous plantation in southeastern China. The main findings can be summarized as follows:

(1) ET declined during the intensive drought period and gradually increased during the recovering drought period. $\lambda E/R_{\mathrm{n}}$, α, Ω, and $\mathrm{WUE_{\_NEP}}$ showed similar seasonal variations as ET, while β and $\mathrm{WUE_{\_GEP}}$ exhibited inverse seasonal variations to ET.

(2) ET and related factors, except $\mathrm{WUE_{\_GEP}}$, were mainly determined by canopy conductance or deep soil water content during the seasonal drought periods. The canopy conductance offset the positive effect of air vapor pressure deficit on ET, $\lambda E/R_{\mathrm{n}}$, and α during the intensive drought period, while the canopy conductance enhanced the positive effect of air temperature on β during the early growing period and on ET and α during the late growing period.

(3) Deep soil water did not satisfy the water needs of ET, and thus stomatal closure and defoliation were adopted by this plantation to cope with drought stress. A time delay effect of precipitation-recovered ET was observed during the recovering drought period.

Acknowledgements. This study was supported by the Strategic Priority Research Program-Climate Change: Carbon Budget and

Relevant Issues of the Chinese Academy of Sciences (Grant No. XDA05050601), the National Natural Science Foundation of China (Grant No. 31070408), and the Strategic Program of Knowledge Innovation of the Chinese Academy of Sciences (Grant No. KZCX2-EW-QN305). The authors thank the anonymous reviewers for their helpful comments and suggestions during peer review.

REFERENCES

Baldocchi, D. D., L. K. Xu, and N. Kiang, 2004: How plant functional-type, weather, seasonal drought, and soil physical properties alter water and energy fluxes of an oak-grass savanna and an annual grassland. *Agricultural and Forest Meteorology*, **123**, 13–39.

Bracho, R., T. L. Powell, S. Dore, J. H. Li, C. R. Hinkle, and B. G. Drake, 2008: Environmental and biological controls on water and energy exchange in Florida scrub oak and pine flatwoods ecosystems. *J. Geophys. Res.*, **113**, G02004, doi: 10.1029/2007jg000469.

Bréda, N., R. Huc, A. Granier, and E. Dreyer, 2006: Temperate forest trees and stands under severe drought: A review of ecophysiological responses, adaptation processes and long-term consequences. *Annals of Forest Science*, **63**, 625–644.

Brümmer, C., and Coauthors, 2012: How climate and vegetation type influence evapotranspiration and water use efficiency in Canadian forest, peatland and grassland ecosystems. *Agricultural and Forest Meteorology*, **153**, 14–30.

Budyko, M. I., 1974: *Climate and Life*. Academic Press, 508 pp.

CFA (China's Forestry Administration), 2005: *Forest Resources of China* 1999–2003. China Forestry Publishing House, 451 pp. (in Chinese)

Churkina, G., D. Schimel, B. H. Braswell, and X. M. Xiao, 2005: Spatial analysis of growing season length control over net ecosystem exchange. *Glob. Change Biol.*, **11**, 1777–1787.

Costa, M. H., M. C. Biajoli, L. Sanches, A. C. M. Malhado, L. R. Hutyra, H. R. da Rocha, R. G. Aguiar, and A. C. de Araújo, 2010: Atmospheric versus vegetation controls of Amazonian tropical rain forest evapotranspiration: Are the wet and seasonally dry rain forests any different? *J. Geophys. Res.*, **115**, G04021, doi: 10.1029/2009jg001179.

da Rocha, H. R., M. L. Goulden, S. D. Miller, M. C. Menton, L. D. V. O. Pinto, H. C. de Freitas, and A. M. e Silva Figueira, 2004: Seasonality of water and heat fluxes over a tropical forest in eastern Amazonia. *Ecological Applications*, **14**, 22–32.

Dairaku, K., S. Emori, and T. Nozawa, 2008: Impacts of global warming on hydrological cycles in the Asian monsoon region. *Adv. Atmos. Sci.*, **25**, 960–973, doi: 10.1007/s00376-008-0960-1.

Falge, E., and Coauthors, 2001: Gap filling strategies for defensible annual sums of net ecosystem exchange. *Agricultural and Forest Meteorology*, **107**, 43–69.

Flanagan, L. B., L. A. Wever, and P. J. Carlson, 2002: Seasonal and interannual variation in carbon dioxide exchange and carbon balance in a northern temperate grassland. *Glob. Change Biol.*, **8**, 599–615.

Goldstein, A. H., and Coauthors, 2000: Effects of climate variability on the carbon dioxide, water, and sensible heat fluxes above a ponderosa pine plantation in the Sierra Nevada (CA). *Agricultural and Forest Meteorology*, **101**, 113–129.

Granier, A. M., and Coauthors, 2007: Evidence for soil water control on carbon and water dynamics in European forests during the extremely dry year: 2003. *Agricultural and Forest Meteorology* **143**, 123–145.

Griffis, T. J., T. A. Black, K. Morgenstern, A. G. Barr, Z. Nesic, G. B. Drewitt, D. Gaumont-Guay, and J. H. McCaughey, 2003: Ecophysiological controls on the carbon balances of three southern boreal forests. *Agricultural and Forest Meteorology*, **117**, 53–71.

Hernández-Santana, V., T. S. David, and J. Martínez-Fernández, 2008: Environmental and plant-based controls of water use in a Mediterranean oak stand. *Forest Ecology and Management*, **255**, 3707–3715.

Hollinger, D. Y., F. M. Kelliher, J. N. Byers, J. E. Hunt, T. M. Mcseveny, and P. L. Weir, 1994: Carbon dioxide exchange between an undisturbed old-growth temperate forest and the atmosphere. *Ecology*, **75**, 134–150.

Huete, A., K. Didan, T. Miura, E. P. Rodriguez, X. Gao, and L. G. Ferreira, 2002: Overview of the radiometric and biophysical performance of the MODIS vegetation indices. *Remote Sens. Environ.*, **83**, 195–213.

Humphreys, E. R., T. A. Black, G. J. Ethier, G. B. Drewitt, D. L. Spittlehouse, E.-M. Jork, Z. Nesic, and N. J. Livingston, 2003: Annual and seasonal variability of sensible and latent heat fluxes above a coastal Douglas-fir forest, British Columbia, Canada. *Agricultural and Forest Meteorology*, **115**, 109–125.

Huxman, T. E., A. A. Turnipseed, J. P. Sparks, P. C. Harley, and R. K. Monson, 2003: Temperature as a control over ecosystem CO_2 fluxes in a high-elevation, subalpine forest. *Oecologia*, **134**, 537–546.

IPCC, 2007: *Climate Change* 2007: *The Physical Science Basis. Working Group* I *Contribution to the Fourth Assessment Report of the Intergovernmental Panel on Climate Change*, Cambridge University Press, New York, 996 pp.

Ishikawa, C., and C. S. Bledsoe, 2000: Seasonal and diurnal patterns of soil water potential in the rhizosphere of blue oaks: Evidence for hydraulic lift. *Oecologia*, **125**, 459–465.

Jarvis, P. G., and K. G. McNaughton, 1986: Stomatal control of transpiration: scaling up from leaf to region. *Advances in Ecological Research*, **15**, 1–49.

Jassal, R. S., T. A. Black, D. L. Spittlehouse, C. Brümmer, and Z. Nesic, 2009: Evapotranspiration and water use efficiency in different-aged Pacific Northwest Douglas-fir stands. *Agricultural and Forest Meteorology*, **149**, 1168–1178.

Kosugi, Y., S. Takanashi, H. Tanaka, S. Ohkubo, M. Tani, M. Yano, and T. Katayama, 2007: Evapotranspiration over a Japanese cypress forest. I. Eddy covariance fluxes and surface conductance characteristics for 3 years. *J. Hydrol.*, **337**, 269–283.

Kumagai, T., T. M. Saitoh, Y. Sato, T. Morooka, O. J. Manfroi, K. Kuraji, and M. Suzuki, 2004: Transpiration, canopy conductance and the decoupling coefficient of a lowland mixed dipterocarp forest in Sarawak, Borneo: Dry spell effects. *J. Hydrol.*, **287**, 237–251.

Leuning, R., H. A. Cleugh, S. J. Zegelin, and D. Hughes, 2005: Carbon and water fluxes over a temperate Eucalyptus forest and a tropical wet/dry savanna in Australia: Measurements and comparison with MODIS remote sensing estimates. *Agricultural and Forest Meteorology*, **129**, 151–173.

Li, Z. H., Y. P. Zhang, S. S. Wang, G. F. Yuan, Y. Yang, and M. Cao, 2010: Evapotranspiration of a tropical rain forest in Xishuangbanna, southwest China. *Hydrological Processes*, **24**, 2405–2416.

Liu, H. Z., G. Tu, C. B. Fu, and L. Q. Shi, 2008: Three-

year variations of water, energy and CO_2 fluxes of cropland and degraded grassland surfaces in a semi-arid area of northeastern China. *Adv. Atmos. Sci.*, **25**, 1009–1020, doi: 10.1007/s00376-008-1009-1.

Malhi, Y., E. Pegoraro, A. D. Nobre, M. G. P. Pereira, J. Grace, A. D. Culf, and R. Clement, 2002: Energy and water dynamics of a central Amazonian rain forest. *J. Geophys. Res.*, **107**, 8061, doi: 10.1029/2001JD000623.

McCaughey, J. H., 1985: Energy-balance storage terms in a mature mixed forest at Petawawa, Ontario—A case-study. *Bound.-Layer Meteor.*, **31**, 89–101.

McNaughton, K. G., and T. W. Spriggs, 1986: A mixed-layer model for regional evaporation. *Bound.-Layer Meteor.*, **34**, 243–262.

Migliavacca, M., and Coauthors, 2009: Seasonal and interannual patterns of carbon and water fluxes of a poplar plantation under peculiar eco-climatic conditions. *Agricultural and Forest Meteorology*, **149**, 1460–1476.

Mishra, A. K., and V. P. Singh, 2010: A review of drought concepts. *J. Hydrol.*, **391**, 202–216.

Monteith, J. L., and M. H. Unsworth, 1990: *Principles of Environmental Physics*. 2nd ed, Chapman and Hall, 291 pp.

Oliphant, A. J., and Coauthors, 2004: Heat storage and energy balance fluxes for a temperate deciduous forest. *Agricultural and Forest Meteorology*, **126**, 185–201.

Reichstein, M., J. D. Tenhunen, O. Roupsard, J. M. Ourcival, S. Rambal, S. Dore, and R. Valentini, 2002: Ecosystem respiration in two Mediterranean evergreen Holm Oak forests: Drought effects and decomposition dynamics. *Functional Ecology*, **16**, 27–39.

Reichstein, M., and Coauthors, 2005: On the separation of net ecosystem exchange into assimilation and ecosystem respiration: review and improved algorithm. *Global Change Biology*, **11**, 1424–1439.

Saigusa, N., and Coauthors, 2010: Impact of meteorological anomalies in the 2003 summer on Gross Primary Productivity in East Asia. *Biogeosciences*, **7**, 641–655.

Schemske, D. W., and C. C. Horvitz, 1988: Plant animal interactions and fruit production in a neotropical herb: A path analysis. *Ecology*, **69**, 1128–1137.

Webb, E. K., G. I. Pearman, and R. Leuning, 1980: Correction of flux measurements for density effects due to heat and water vapour transfer. *Quart. J. Roy. Meteor. Soc.*, **106**, 85–100.

Wen, X. F., H. M. Wang, J. L. Wang, G. R. Yu, and X. M. Sun, 2010: Ecosystem carbon exchanges of a subtropical evergreen coniferous plantation subjected to seasonal drought, 2003–2007. *Biogeosciences*, **7**, 357–369.

Wilczak, J. M., S. P. Oncley, and S. A. Stage, 2001: Sonic anemometer tilt correction algorithms. *Bound.-Layor. Meteor.*, **99**, 127–150.

Wilson, K. B., and D. D. Baldocchi1, 2000: Seasonal and interannual variability of energy fluxes over a broadleaved temperate deciduous forest in North America. *Agricultural and Forest Meteorology*, **100**, 1–18.

Wilson, K. B., and Coauthors, 2002: Energy partitioning between latent and sensible heat flux during the warm season at FLUXNET sites. *Water Resour. Res.*, **38**, 30-1–30-11.

Zhang, W. J., H. M. Wang, X. F. Wen, F. T. Yang, Z. Q. Ma, X. M. Sun, and G. R. Yu, 2011: Freezing-induced loss of carbon uptake in a subtropical coniferous plantation in southern China. *Annals of Forest Science*, **68**, 1151–1161.